Received April 27, 2019, accepted May 11, 2019, date of publication May 15, 2019, date of current version June 21, 2019.

*Digital Object Identifier 10.1109/ACCESS.2019.2916785*

# Fault Detection for Closed-Loop Control Systems Based on Parity Space Transformation

**BOWEN SUN[1], JIONGQI WANG[1], ZHANGMING HE[1,3], YONGRUI QIN[2,4], DAYI WANG[3], AND HAIYIN ZHOU[1]**

[1]College of Liberal Arts and Sciences, National University of Defense Technology, Changsha, 410073, China
[2]School of Electronic Information Engineering, Guangdong University of Petrochemical Technology, Maoming 525000, China
[3]Beijing Institute of Spacecraft System Engineering, China Academy of Space Technology, Beijing 100094, China
[4]School of Computing and Engineering, University of Huddersfield, West Yorkshire HD1 3DH, U.K.

Corresponding author: Jiongqi Wang (wjq_gfkd@163.com)

This work was supported in part by the National Natural Science Foundation of China under Grant 61773021, in part by the National Natural Science Fund for Distinguished Young Scholars of China under Grant 61525301, in part by the Natural Science Foundation of Hunan Province under Grant 2019JJ20018 and Grant 2019JJ50745, and in part by the Science and Technology on Space Intelligent Control Laboratory under Grant HTKJ2019KL5502007.

**ABSTRACT** Fault detection for closed-loop control systems is the future development in the field of the fault diagnosis. Since a closed-loop control system is generally very robust to the external disturbances, fault detection has been challenging a hot research area. Traditional data-driven detection methods are not particularly designed for closed-loop control systems and thus can be improved. In this paper, a new fault detection method is proposed, which is based on the parity space for the closed-loop control system. The main principle of our method is to transform the detection residual into the parity space of the original space to restrict false detection or leak detection caused by the estimation of uncertain states. More specifically, the construction of the stable kernel matrix in the parity space is given, and the residual sequence is accumulated to improve the fault-to-noise ratio and thus increase the detection performance. To verify our method, we have conducted a simulation which is based on a numerical simulation model and the Tennessee industrial system respectively. The results show that the proposed method is more feasible and more effective in fault detection for closed-loop control systems compared with the traditional data-driven detection methods, including the time series modeling method and the partial least squares method.

**INDEX TERMS** Fault detection, closed-loop control, parity space, stable kernel matrix, detection performance.

## I. INTRODUCTION

With the development of science and technology, the complexity of the industrial systems has been increasing. The fault of these complex systems can lead to the decline in the product quality and may cause significant property damage or casualties [1]. Therefore, it has become the research focus to improve the safety and the reliability of the system operation and to detect the fault timely and accurately [2].

In order to achieve the predetermined production goals or to meet the stability and the robustness for the industrial systems, the closed control loop is generally applied. Through the closed control loop, the influence of external disturbance on the operation of the system is reduced, which makes the system much more robust. At present, a large number of closed control loops have been widely used in the industrial production processes [3], such as proportional integral differential control, optimal control, robust control, etc.

Due to the nature of closed control loops, the performance of fault detection and diagnosis is degraded. The main reasons are as follows [4]:

1) In terms of fault detection, the closed control loop usually makes the system more robust to the external disturbances. Therefore, when the fault happens in the early stage or the fault magnitude is small, the fault signal will be covered by the external control signal, which is difficult for the fault to be detected, resulting in lower fault detection rate;

2) In terms of fault identification, the closed control loop will encourage the fault to propagate inside the system, leading to the faults existing in many variables/signals. Such fault transmission phenomenon increases the difficulty for fault identification.

The associate editor coordinating the review of this manuscript and approving it for publication was Guangdeng Zong.

This paper focuses on addressing fault detection issues in closed-loop control systems. The main aim is to achieve fault detection in closed-loop control systems and improve fault detection performance.

There have been a lot of research results in the area of fault detection for open-loop systems [5]–[10]. However, due to the nature of closed control loops, the operating characteristics of closed-loop control systems are significantly different from open-loop systems, and the closed-loop control system is generally much more robust and stable. Therefore, most of existing fault detection methods for open-loop systems cannot be directly applied to closed-loop control systems.

To be more specific, the difficulty of fault detection in closed-loop control systems is mainly due to the following facts: (1) The closed control loop makes the fault magnitude smaller, therefore the detection residual constructed by traditional methods is unable to meet relevant detection requirements [11]–[13]; (2) The dynamicity of the system poses great challenges in constructing the accurate model and determining the model parameters, leading to the consequence that state vectors cannot be estimated accurately.

In a word, the closed-loop control system can reduce the external disturbance, so that the fault could be overwhelmed by the noise, which brings difficulties to the fault detection. Based on these observations, in this paper, we propose to increase fault-to-noise ratios through the accumulation of the residual sequence and to construct the detection residual when the fault magnitude is small in close-loop control systems. Besides, we adopt the parity space transformation to change the characters of the detection residual when the model state is not clear or the model parameters are unknown, aiming to improve the fault detection performance.

The main contributions of this paper are as follows: Firstly, the parity space transformation is adapted and applied in the fault detection of the closed-loop control systems, which can solve the uncertain estimation of the state vector for the fault detection in closed-loop control systems and improve fault detection rates. Secondly, for the parity space transformation, a more effective method for selecting a stable kernel matrix is designed, which can obtain much more accurate parity space. Thirdly, when dealing with the problem that the system fault amplitude becomes smaller in the closed control loop, the residual sequence in the time window is used to construct new detection residuals for enhancing the fault-to-noise ratio and improving the fault detection rate. Finally, the improved fault detection method is applied to both the numerical simulation system and the Tennessee industrial system to implement and verify fault detection in closed-loop control systems.

The remainder of this paper is organized as follows: In Section II, we introduce the related works. In Section III, the parity space principle is introduced, and a classic construction method of detection residuals and stable kernel matrix are also described. Section IV firstly presents a straightforward fault detection method based on the parity space in a closed-loop control system, and then develops an improved fault detection method with a technique of accumulating residuals for systems with smaller fault-to-noise ratios. Section V presents experiments on both the numerical simulation model systems and the Tennessee industrial systems, and the results are reported and discussed. Finally, the conclusion is drawn in Section VI.

## II. RELATED WORK

At present, there are a lot of research results in fault detection for open-loop systems [5]–[10].

The impact of fault detection on a lab-scale electric machine system was studied [14]. Under the open-loop control system, the torque current power spectrum can be used to detect the electrical faults. Nevertheless, in closed-loop control systems, the frequency features are covered by the control signal. Therefore, the fault detection methods for open-loop systems cannot be used for closed-loop control systems directly.

When the system model and its parameters are certain, the traditional model-based fault detection methods usually use the calculated value of the model and the output value of the actual system to construct the residual statistic to realize the fault detection [15]–[17]. While in the closed-loop control systems [18], [19], the system residuals may tend to zero because of the designed closed control loop [20]. Therefore, the system residuals are not sensitive to detect the faults in closed-loop control systems, which will increase the fault detection difficulties.

Due to the complexity of the practical system, it is difficult to establish the accurate system model [21]. Besides, to establish a complete fault model database is also too expensive. Therefore, when the system model is uncertain, the data-driven fault detection methods are generally selected. In open-loop systems, the research results based on the data-driven fault detection methods are also significant. However, due to the inherent characteristics of closed-loop control systems, most of the data-driven detection methods for open-loop systems are also difficult to be directly applied to closed-loop control systems.

The fault detection methods based on the time series was proposed in Reference [22], [23]. The ARMA model aims at predicting the current measurement value through the historical measurement values and the corresponding noise. The closed-loop control system will make the fault magnitude tend to zero, which cannot distinguish the noise from the fault well. Therefore, the time series modeling method cannot be applied to the fault detection in closed-loop control systems.

The fault detection method based on the Partial Least Squares (PLS) was studied [24], [25]. This method combines the idea of the Principal Component Analysis (PCA) and the Canonical Correlation Analysis (CCA) to find the relationship between the input data and the output data of the system. And this method works well in the static data detection. However, the data will not be static due to the closed control loop in the close-loop control systems. Besides, there is a strong correlation among the data, which makes the PLS method cannot handle well for closed-loop control systems. In addition, the PLS needs to estimate the state vector accurately to construct the detection residuals. When the state vector cannot be accurately estimated, the method will break down.

The fault detection for the sensor faults in the linear closed-loop dynamic systems was studied with the multiple inputs and the multiple outputs [26]. A classification method based on the data-driven residual generators was proposed. Since it is necessary to seek the proportional relationship among the measured data and to estimate the relationship by the least squares method, the initial state vector of the system must be ignored, which has a great influence on the prediction accuracy, thus affects the detection result.

The parity space is an abstract expression of the vector space relationship and any vector space has its corresponding parity space. The parity space corresponding to the original vector space can be found through the parity space transformation. The parity space is orthogonal to the original vector space. Besides, it can be directly connected to the original space to construct the full space. In this way, some spatial characteristics in the original vector space are better reflected in its parity space [2], [20].

According to the statement above, this paper aims at solving the problem of fault detection in closed-loop control systems. With the parity space transformation, it can effectively solve the problem of the fault alarm or the missed detection due to the inaccurate estimation for the state vector. Through the data characteristics in the parity space, the change of detection residuals can be calculated in the parity space. Then the fault in the closed-loop control system can be detected.

## III. PRINCIPLE OF PARITY SPACE

### A. CONSTRUCTION OF DETECTION RESIDUALS

Firstly, we establish a discrete linear model for the a control system as follows:

$$\begin{cases} \boldsymbol{x}_{k+1} = \boldsymbol{A}\boldsymbol{x}_k + \boldsymbol{B}\boldsymbol{u}_k + \boldsymbol{f}_k^x + \boldsymbol{w}_k \\ \boldsymbol{y}_k = \boldsymbol{C}\boldsymbol{x}_k + \boldsymbol{f}_k^y + \boldsymbol{v}_k \end{cases} \tag{1}$$

where $\boldsymbol{x}_k \in \mathbb{R}^{n_x}$ is the state vector, $\boldsymbol{u}_k \in \mathbb{R}^{n_u}$ is the input vector, $\boldsymbol{y}_k \in \mathbb{R}^{n_y}$ is the output vector, $\boldsymbol{w}_k \in \mathbb{R}^{n_x}$ and $\boldsymbol{v}_k \in \mathbb{R}^{n_y}$ are the independent process noise and the measurement noise, with zero mean, and the covariance matrices are the normal distribution of $\boldsymbol{Q} \in \mathbb{R}^{n_x \times n_x}$ and $\boldsymbol{R} \in \mathbb{R}^{n_y \times n_y}$ respectively; $\boldsymbol{f}_k^x \in \mathbb{R}^{n_x}$ and $\boldsymbol{f}_k^y \in \mathbb{R}^{n_y}$ are the actuator fault and the sensor fault (When the system operates normally, i.e., $\boldsymbol{f}_k^x = \boldsymbol{0}$ and $\boldsymbol{f}_k^y = \boldsymbol{0}$); $\boldsymbol{A}, \boldsymbol{B}, \boldsymbol{C}$ are the parameter matrices with appropriate dimensions, which are all unknown.

For Model (1), if we unite the measurement data of $q$ moments to rearrange the sampled data, and let $\boldsymbol{Y}_{k,q} = \left[\boldsymbol{y}_k, \boldsymbol{y}_{k+1}, \ldots, \boldsymbol{y}_{k+q-1}\right]^{\mathrm{T}}$, then we have another model as follows:

$$\begin{aligned} \boldsymbol{Y}_{k,q} &= \boldsymbol{\Gamma}_q \boldsymbol{x}_k + \boldsymbol{\Theta}_{u,q}\boldsymbol{U}_{k-1,q} \\ &\quad + \boldsymbol{\Theta}_{w,q}\boldsymbol{W}_{k-1,q} + \boldsymbol{V}_{k,q} + \boldsymbol{\Theta}_{f,q}\boldsymbol{F}_{k,q}^x + \boldsymbol{F}_{k,q}^y \end{aligned} \tag{2}$$

where $\boldsymbol{U}_{k-1,q} = \left[\boldsymbol{u}_{k-1}, \boldsymbol{u}_k, \cdots, \boldsymbol{u}_{k+q-2}\right]^{\mathrm{T}}$,

$$\begin{aligned}
\boldsymbol{W}_{k-1,q} &= \left[\boldsymbol{w}_{k-1}, \boldsymbol{w}_k, \cdots, \boldsymbol{w}_{k+q-2}\right]^{\mathrm{T}}, \\
\boldsymbol{V}_{k,q} &= \left[\boldsymbol{v}_k, \boldsymbol{v}_{k+1}, \cdots, \boldsymbol{v}_{k+q-1}\right]^{\mathrm{T}}, \\
\boldsymbol{F}_{k,q}^x &= \left[\boldsymbol{f}_k^x, \boldsymbol{f}_{k+1}^x, \cdots, \boldsymbol{f}_{k+q-1}^x\right]^{\mathrm{T}}, \\
\boldsymbol{F}_{k,q}^y &= \left[\boldsymbol{f}_k^y, \boldsymbol{f}_{k+1}^y, \cdots, \boldsymbol{f}_{k+q-1}^y\right]^{\mathrm{T}}, \\
\boldsymbol{\Gamma}_q &= \left[\left(\boldsymbol{C}\boldsymbol{A}^0\right)^{\mathrm{T}}, \left(\boldsymbol{C}\boldsymbol{A}^1\right)^{\mathrm{T}}, \ldots, \left(\boldsymbol{C}\boldsymbol{A}^{q-1}\right)^{\mathrm{T}}\right]^{\mathrm{T}} \in \mathbb{R}^{qn_y \times n_x},
\end{aligned}$$

$$\boldsymbol{\Theta}_{u,q} = \begin{bmatrix} \boldsymbol{C}\boldsymbol{A}^0\boldsymbol{B} & \boldsymbol{0} & \cdots & \boldsymbol{0} \\ \boldsymbol{C}\boldsymbol{A}\boldsymbol{B} & \boldsymbol{C}\boldsymbol{A}^0\boldsymbol{B} & \ddots & \vdots \\ \vdots & \ddots & \ddots & \boldsymbol{0} \\ \boldsymbol{C}\boldsymbol{A}^{q-1}\boldsymbol{B} & \cdots & \boldsymbol{C}\boldsymbol{A}\boldsymbol{B} & \boldsymbol{C}\boldsymbol{A}^0\boldsymbol{B} \end{bmatrix} \in \mathbb{R}^{qn_y \times qn_u},$$

$$\boldsymbol{\Theta}_{w,q} = \begin{bmatrix} \boldsymbol{C}\boldsymbol{A}^0 & \boldsymbol{0} & \cdots & \boldsymbol{0} \\ \boldsymbol{C}\boldsymbol{A} & \boldsymbol{C}\boldsymbol{A}^0 & \ddots & \vdots \\ \vdots & \ddots & \ddots & \boldsymbol{0} \\ \boldsymbol{C}\boldsymbol{A}^{q-1} & \cdots & \boldsymbol{C}\boldsymbol{A} & \boldsymbol{C}\boldsymbol{A}^0 \end{bmatrix} \in \mathbb{R}^{qn_y \times qn_w},$$

$$\boldsymbol{\Theta}_{f,q} = \begin{bmatrix} \boldsymbol{0} & \boldsymbol{0} & \cdots & \boldsymbol{0} \\ \boldsymbol{C}\boldsymbol{A}^0 & \boldsymbol{0} & \ddots & \vdots \\ \vdots & \ddots & \ddots & \boldsymbol{0} \\ \boldsymbol{C}\boldsymbol{A}^{q-2} & \cdots & \boldsymbol{C}\boldsymbol{A}^0 & \boldsymbol{0} \end{bmatrix} \in \mathbb{R}^{qn_y \times qn_w}$$

In Model (2), the state vector $\boldsymbol{x}_k$ cannot be accurately obtained, therefore if the state vector can be eliminated, the accuracy of the fault detection can be improved.

The state vector in Model (2) can be eliminated through the parity space transformation, that is to calculate $\boldsymbol{\Gamma}_q^{\perp}$, which is the left null space of $\boldsymbol{\Gamma}_q$. Furthermore, the left null space $\boldsymbol{\Gamma}_q^{\perp}$ should satisfy that $\boldsymbol{\Gamma}_q^{\perp}\boldsymbol{\Gamma}_q = \boldsymbol{0}$ and the two matrices can be extended to the full space. Hence, in Model (2), if we multiply both sides by $\boldsymbol{\Gamma}_q^{\perp}$, then we have

$$\begin{aligned} &\boldsymbol{\Gamma}_q^{\perp}\boldsymbol{Y}_{k,q} \\ &= \boldsymbol{\Gamma}_q^{\perp}\left(\boldsymbol{\Theta}_{u,q}\boldsymbol{U}_{k-1,q} + \boldsymbol{\Theta}_{w,q}\boldsymbol{W}_{k-1,q} + \boldsymbol{V}_{k,q} + \boldsymbol{\Theta}_{f,q}\boldsymbol{F}_{k,q}^x + \boldsymbol{F}_{k,q}^y\right) \end{aligned} \tag{3}$$

Further, Eq. (3) can be rewritten as

$$\begin{aligned} &\boldsymbol{\Gamma}_q^{\perp}\boldsymbol{Y}_{k,q} - \boldsymbol{\Gamma}_q^{\perp}\boldsymbol{\Theta}_{u,q}\boldsymbol{U}_{k-1,q} \\ &\quad = \boldsymbol{\Gamma}_q^{\perp}\left(\boldsymbol{\Theta}_{w,q}\boldsymbol{W}_{k-1,q} + \boldsymbol{V}_{k,q} + \boldsymbol{\Theta}_{f,q}\boldsymbol{F}_{k,q}^x + \boldsymbol{F}_{k,q}^y\right) \end{aligned} \tag{4}$$

Let

$$\begin{cases} \boldsymbol{\Phi} = \begin{bmatrix} -\boldsymbol{\Gamma}_q^{\perp}\boldsymbol{\Theta}_{u,q} & \boldsymbol{\Gamma}_q^{\perp} \end{bmatrix} \\ \boldsymbol{z}_{k,q} = \begin{bmatrix} \boldsymbol{U}_{k-1,q}^{\mathrm{T}} & \boldsymbol{Y}_{k,q}^{\mathrm{T}} \end{bmatrix}^{\mathrm{T}} \\ \boldsymbol{r}_{k,q} = \boldsymbol{\Phi}\boldsymbol{z}_{k,q} \end{cases} \tag{5}$$

where $\boldsymbol{\Phi}$ is the stable kernel matrix of the parity space transformation. When the system operates normally, i.e., $\boldsymbol{F}_{k,q}^x = 0$

and $\boldsymbol{F}^y_{k,q} = 0$, we have

$$\boldsymbol{r}_{k,q} = \boldsymbol{\Gamma}_q^{\perp}\left(\boldsymbol{\Theta}_{w,q}\boldsymbol{W}_{k-1,q} + \boldsymbol{V}_{k,q}\right) \tag{6}$$

It should be noted that the residual follows the normal distribution with zero mean. Then we have the covariance matrix as $\boldsymbol{\Sigma} = \boldsymbol{\Gamma}_q^{\perp}\boldsymbol{\Theta}_{w,q}\boldsymbol{Q}\left(\boldsymbol{\Gamma}_q^{\perp}\boldsymbol{\Theta}_{w,q}\right)^{\mathrm{T}} + \boldsymbol{\Gamma}_q^{\perp}\boldsymbol{R}\left(\boldsymbol{\Gamma}_q^{\perp}\right)^{\mathrm{T}}$, i.e., $\boldsymbol{r}_{k,q} \sim N(\boldsymbol{0}, \boldsymbol{\Sigma})$ when the system operates normally; if a fault occurs, the residuals can be represented as

$$\boldsymbol{r}_{k,q} = \boldsymbol{\Gamma}_q^{\perp}\left(\boldsymbol{\Theta}_{w,q}\boldsymbol{W}_{k-1,q} + \boldsymbol{V}_{k,q} + \boldsymbol{\Theta}_{f,q}\boldsymbol{F}^x_{k,q} + \boldsymbol{F}^y_{k,q}\right) \tag{7}$$

and then the expectation of the residual will deviate from zero.

### B. ESTABLISHMENT OF STABLE KERNEL MATRIX

The matrix $\boldsymbol{\Phi}$ is an important operator for the parity space transformation, and its choice has a great influence on the structure and the characteristics of the constructed parity space. Here, a stable kernel matrix can play a critical role in the parity space transformation. There have been quite a few research efforts in mathematics on how to derive a stable kernel matrix [2], [27], [28].

When the system operates normally, $\mathrm{E}\boldsymbol{r}_{k,q} = \mathrm{E}\boldsymbol{\Phi}\boldsymbol{z}_{k,q} = \boldsymbol{0}$ for Eq. (5) and Eq. (6). Therefore, the stable kernel matrix $\boldsymbol{\Phi}$ can be obtained with the training data from the normal operating system. Assume that the total number of the training samples is $\tilde{N}$, let $N = \tilde{N} - q$, then we have

$$\boldsymbol{Z}_N = \begin{bmatrix} \boldsymbol{U}_{1,q} & \boldsymbol{U}_{2,q} & \cdots & \boldsymbol{U}_{N-1,q} \\ \boldsymbol{Y}_{2,q} & \boldsymbol{Y}_{3,q} & \cdots & \boldsymbol{Y}_{N,q} \end{bmatrix} \in \mathbb{R}^{q(n_u+n_y)\times(N-1)} \tag{8}$$

We apply the singular value decomposition (SVD) for the training data set $\boldsymbol{Z}_N$

$$\boldsymbol{Z}_N = \begin{bmatrix} \boldsymbol{H}_1 & \boldsymbol{H}_2 \end{bmatrix} \begin{bmatrix} \boldsymbol{\Lambda}_1 & \\ & \boldsymbol{\Lambda}_2 \end{bmatrix} \begin{bmatrix} \boldsymbol{P}_1 & \boldsymbol{P}_2 \end{bmatrix}^{\mathrm{T}} \tag{9}$$

Let $n_r = qn_y - n_x > 0$, where $\boldsymbol{\Lambda}_2 \in \mathbb{R}^{n_r\times n_r}$, $\boldsymbol{P}_2 \in \mathbb{R}^{q(n_u+n_y)\times n_r}$, $\boldsymbol{H}_2 \in \mathbb{R}^{q(n_u+n_y)\times n_r}$. Since the matrix $\begin{bmatrix} \boldsymbol{H}_1 & \boldsymbol{H}_2 \end{bmatrix}$ is a unitary matrix, Eq. (9) can be rewritten as

$$\begin{bmatrix} \boldsymbol{H}_1^{\mathrm{T}} \\ \boldsymbol{H}_2^{\mathrm{T}} \end{bmatrix} \boldsymbol{Z}_N = \begin{bmatrix} \boldsymbol{\Lambda}_1 & \\ & \boldsymbol{\Lambda}_2 \end{bmatrix} \begin{bmatrix} \boldsymbol{P}_1^{\mathrm{T}} \\ \boldsymbol{P}_2^{\mathrm{T}} \end{bmatrix} \tag{10}$$

Through calculating the rank of the matrix $\boldsymbol{Z}_N$, the singular value $\boldsymbol{\Lambda}_2 \approx \boldsymbol{0}$. Then $\boldsymbol{H}_2$ can be expanded into the parity space of the training data set $\boldsymbol{Z}_N$, which is

$$\boldsymbol{H}_2^{\mathrm{T}}\boldsymbol{z}_{k,q} = \boldsymbol{\Lambda}_2\boldsymbol{P}_2^{\mathrm{T}} \approx \boldsymbol{0} \tag{11}$$

Then the stable kernel matrix $\boldsymbol{\Phi}$ is established, and $\boldsymbol{\Phi} = \boldsymbol{H}_2^{\mathrm{T}}$.

### C. EXISTENCE OF STABLE KERNEL MATRIX

According to Model (2), the observed sequence vector $\boldsymbol{Y}_{k,q}$ can be written as a linear combination of the input sequence vector $\boldsymbol{U}_{k-1,q}$ and the state vector $\boldsymbol{x}_k$. If the system has no noise, combining with Eq. (8), the following equation can be obtained:

$$\boldsymbol{Z}_N = \begin{bmatrix} \boldsymbol{E} & \boldsymbol{0} \\ \boldsymbol{\Theta}_{u,q} & \boldsymbol{\Gamma}_q \end{bmatrix} \begin{bmatrix} \boldsymbol{U}_{1,q} & \boldsymbol{U}_{2,q} & \cdots & \boldsymbol{U}_{N-1,q} \\ \boldsymbol{x}_2 & \boldsymbol{x}_3 & \cdots & \boldsymbol{x}_N \end{bmatrix} \tag{12}$$

Because the matrix $\begin{bmatrix} \boldsymbol{E} & \boldsymbol{0} \\ \boldsymbol{\Theta}_{u,q} & \boldsymbol{\Gamma}_q \end{bmatrix}$ is of full column rank, the rank of

$$rank\left(\begin{bmatrix} \boldsymbol{U}_{1,q} & \boldsymbol{U}_{2,q} & \cdots & \boldsymbol{U}_{N-1,q} \\ \boldsymbol{x}_2 & \boldsymbol{x}_3 & \cdots & \boldsymbol{x}_N \end{bmatrix}\right) = qn_u + n_x$$

according to Eq. (12). The number of rows of the matrix $\boldsymbol{Z}_N$ is $qn_u + qn_y$, and the last $qn_y - n_x$ items for the singular values of the matrix $\boldsymbol{Z}_N$ are zero, which is $\boldsymbol{\Lambda}_2 = \boldsymbol{0}$. Due to the noise, the singular values $\boldsymbol{\Lambda}_2 \approx \boldsymbol{0}$ in practice, we only need to select the value of the appropriate sampling number $q$, so that $qn_y - n_x > 0$, then we can ensure that the stable kernel matrix $\boldsymbol{\Phi}$ exists.

## IV. FAULT DETECTION BASED ON PARITY SPACE FOR CLOSED-LOOP SYSTEM

### A. LINEAR MODEL FOR CLOSED-LOOP SYSTEM

If we add the closed control loop into Model (1), the closed-loop control system equation can be written as

$$\begin{cases} \boldsymbol{x}_{k+1} = \boldsymbol{A}\boldsymbol{x}_k + \boldsymbol{B}\boldsymbol{u}_k + \boldsymbol{w}_k + \boldsymbol{f}^x_k \\ \boldsymbol{y}_k = \boldsymbol{C}\boldsymbol{x}_k + \boldsymbol{v}_k + \boldsymbol{f}^y_k \\ \boldsymbol{x}^c_{k+1} = \boldsymbol{A}^c\boldsymbol{x}^c_k + \boldsymbol{B}^c\boldsymbol{y}_k \\ \boldsymbol{u}_k = \boldsymbol{C}^c\boldsymbol{x}^c_k + \boldsymbol{D}^c\boldsymbol{y}_k \end{cases} \tag{13}$$

where $\boldsymbol{x}^c_k \in \mathbb{R}^{n_{xc}}$ is the state control vector, $\boldsymbol{A}^c, \boldsymbol{B}^c, \boldsymbol{C}^c, \boldsymbol{D}^c$ are the parameter matrices with appropriate dimensions. It is worth noting that, because of the closed control loop, the measured output will affect the input value at the next moment. If the feedback control is a negative feedback, the fault amplitude will be reduced, which brings the difficulties for fault detection.

### B. STABLE KERNEL MATRIX FOR A CLOSED-LOOP CONTROL SYSTEM

Similar to Eq. (2), without considering the closed control loop, the formula can be obtained when the system operates normally as follows:

$$\boldsymbol{Y}_{k,q} = \boldsymbol{\Gamma}_q\boldsymbol{x}_k + \boldsymbol{\Theta}_{u,q}\boldsymbol{U}_{k-1,q} + \boldsymbol{\Theta}_{w,q}\boldsymbol{W}_{k-1,q} + \boldsymbol{V}_{k,q} \tag{14}$$

According to the parity space transformation introduced in Section III, if the stable kernel matrix $\boldsymbol{\Phi}$ can be obtained, the residual at each moment can be calculated through Eq. (5). Once we successfully calculate the residual characteristics according to the training data under the normal conditions and combine the detection statistics with the corresponding detection thresholds, we can then judge whether the faults occur or not.

Unlike an open-loop control system, in a closed-loop control system, the measured data $\boldsymbol{Y}$ also affects the input data $\boldsymbol{U}$. However, in such situation, the rank of the data set may become smaller. If we completely adopt the method described in Section III to obtain the stable kernel matrix $\mathbf{\Phi}$, it may further compress the residuals in the parity space and the performance for the fault detection will be decreased.

Similar to Eq. (14), consider the equation of the input data and the output data with the closed control loop as follows:

$$\boldsymbol{U}_{k,q} = \tilde{\mathbf{\Gamma}}_q \boldsymbol{x}_k^c + \mathbf{\Theta}_{y,q} \boldsymbol{Y}_{k,q} \tag{15}$$

where $\boldsymbol{U}_{k,q}$ and $\boldsymbol{Y}_{k,q}$ are the output data and the input data of the closed-loop control system respectively, whose symbol form is similar to that in Eq. (2), which can be demonstrated as follows:

$$\mathbf{\Theta}_{y,q} = \begin{bmatrix} \boldsymbol{D}^c & \mathbf{0} & \cdots & \mathbf{0} \\ \boldsymbol{C}^c\boldsymbol{B}^c & \boldsymbol{D}^c & \cdots & \mathbf{0} \\ \vdots & \vdots & \ddots & \vdots \\ \boldsymbol{C}^c(\boldsymbol{A}^c)^{q-2}\boldsymbol{B}^c & \boldsymbol{C}^c(\boldsymbol{A}^c)^{q-3}\boldsymbol{B}^c & \cdots & \boldsymbol{D}^c \end{bmatrix} \in \mathbb{R}^{qn_u \times qn_y},$$

$$\tilde{\mathbf{\Gamma}}_q = \begin{bmatrix} \boldsymbol{C}^c \\ \boldsymbol{C}^c\boldsymbol{A}^c \\ \vdots \\ \boldsymbol{C}^c(\boldsymbol{A}^c)^{q-1} \end{bmatrix} \in \mathbb{R}^{qn_u \times n_{x^c}}.$$

It can be seen from Eq. (15) that the input data in the closed-loop control system is affected by both the output data and the state control vector. Consider the training data set for Eq. (8) constructed in Section III, The rank of the matrix $\boldsymbol{Z}_N$ can be determined by the state vector $\boldsymbol{x}_k$, the state control vector $\boldsymbol{x}_k^c$ and the $k$-time input $\boldsymbol{u}_k$, i.e., *rank* $(\boldsymbol{Z}_N) = n_x + n_{x^c} + n_u$. Now the rank of the parity space is not $qn_y - n_x$, and actually it becomes $n_r = qn_y + (q-1)\, n_u - n_x - n_{x^c}$.

In essence, the parity space method finds the left null space. Since the matrix $\boldsymbol{Z}_N$ in Eq. (12) is not full of rank, the projection in the left null space can be regarded as the system residuals, that is, the projection of noise in this space. Then calculate the statistical characteristics of the residuals for fault detection.

## C. IMPROVEMENT FOR CONSTRUCTING DETECTION RESIDUAL

In the closed-loop control system, since the output vector has a feedback adjustment function to the system, it generally counteracts the external disturbance. However, its effect on the white Gaussian noise is opposite, which may increase the variance of the noise. On the other hand, when the fault occurs in the closed-loop control system, the fault magnitude will become smaller due to the closed control loop. Because of the above reasons, the fault-to-noise ratio will be reduced and the difficulty of the fault detection will increase, which is a key problem of fault detection in closed-loop control systems.

When detecting the fault based on the parity space transformation, the problem above may also exist. In this case, the residual with only a single moment is not enough for fault detection, but it can increase the fault-to-noise ratio by accumulating the residual sequence of a sliding window to construct an improved residual with a higher fault-to-noise ratio, which can improve the fault detection performance. However, the real-time performance of the fault detection may not achieve the best results due to the accumulation of the residual sequence.

Take a one-dimensional fault as an example, and let the fault magnitude be $f_k$ at $k$-time. When the system operates normally, the residual $r_k$ follows the distribution as follows:

$$r_k \sim N\left(0, \tilde{\Sigma}\right) \tag{16}$$

where $\tilde{\Sigma}$ is the variance of the residual $r_k$, and when the fault occurs, the residual $r_k$ follows the distribution as follows

$$r_k \sim N\left(f_k, \tilde{\Sigma}\right) \tag{17}$$

The fault is easily overwhelmed by the noise with a lower fault-to-noise ratio, which makes it difficult to detect the fault accurately. If we accumulate the $N_0$ residuals in a sliding window, then

$$\tilde{r}_k = \sum_{j=k-N_0+1}^{k} r_j \tag{18}$$

Now the residual follows the distribution as follows

$$\tilde{r}_k \sim N\left(\sum_{j=k-N_0+1}^{k} f_j, N_0\tilde{\Sigma}\right) \tag{19}$$

Now the fault-to-noise ratio is $\left|\sum_{j=k-N_0+1}^{k} f_j \Big/ \sqrt{N_0\tilde{\Sigma}}\right|$, which is increased obviously.

According to the above analysis, the fault detection performance can be improved by appropriately increasing the detection delay. However, the above method is not suitable for sudden faults, and currently there is no appropriate solution for sudden fault detection with a small magnitude.

## D. DETECTION STATISTICS AND DETECTION PERFORMANCE

If $\tilde{\boldsymbol{r}}_k$,the sum of the $N_0$ residuals $\boldsymbol{r}_j$, can be calculated (as shown in Eq. (18)), where $k$ represents the current moment, then the statistical characteristics from the training data can be used to detect fault in the test data.

Assume that the sample number of the improved residuals is $N-k+1$, let

$$\boldsymbol{R} = \begin{bmatrix} \tilde{\boldsymbol{r}_k} & \tilde{\boldsymbol{r}_{k+1}} & \cdots & \tilde{\boldsymbol{r}_N} \end{bmatrix} \tag{20}$$

We can calculate the covariance matrix of the training data as follows:

$$\boldsymbol{S} = \frac{1}{N-k}\boldsymbol{R}\boldsymbol{R}^{\mathrm{T}} \tag{21}$$

As for the improved residual $\tilde{\boldsymbol{r}}$ from the test data, the $T^2$ statistics can be computed as

$$T^2 = \tilde{\boldsymbol{r}}^{\mathrm{T}}\boldsymbol{S}^{-1}\tilde{\boldsymbol{r}} \tag{22}$$

The $T^2$ statistics obeys $F$-distribution in the normal system [29]. Let $\hat{N} = N - k + 1$ and the threshold is as follows

$$T_\alpha^2 = \frac{m\left(\hat{N}-1\right)\left(\hat{N}+1\right)}{\hat{N}\left(\hat{N}-m\right)} F_\alpha\left(m, \hat{N}-m\right) \tag{23}$$

where $m = row\left(\boldsymbol{R}\right)$ is the dimension of the measurement space.

*Proof:* Consider $\boldsymbol{R} = \left[\tilde{\boldsymbol{r}}_k, \tilde{\boldsymbol{r}}_{k+1}, \cdots, \tilde{\boldsymbol{r}}_N\right]^T$, $\tilde{\boldsymbol{r}}_i \overset{iid}{\sim} N\left(\boldsymbol{0}, \widehat{\boldsymbol{\Sigma}}\right), i = k, \cdots, N$, and then the matrix $\boldsymbol{S} = \frac{1}{N-k}\boldsymbol{R}\boldsymbol{R}^T$ obey the Wishart distribution (W-distribution).

So let

$$\begin{cases} z_i = \sqrt{\dfrac{\hat{N}}{\hat{N}+1}}\boldsymbol{\Sigma}^{1/2}\tilde{\boldsymbol{r}}_i \overset{iid}{\sim} N\left(\boldsymbol{0}, \boldsymbol{I}\right), & i = k, \cdots, N \\ \boldsymbol{W} = \left(\hat{N}-1\right)\boldsymbol{\Sigma}^{-1/2}\boldsymbol{S}^{-1}\boldsymbol{\Sigma}^{-1/2} & \end{cases} \tag{24}$$

So

$$\begin{aligned} &\frac{\hat{N}\left(\hat{N}-m\right)}{m\left(\hat{N}^2-1\right)}\tilde{\boldsymbol{r}}^T\boldsymbol{S}^{-1}\tilde{\boldsymbol{r}} \\ &\quad = \frac{\hat{N}\left(\hat{N}-m\right)}{m\left(\hat{N}^2-1\right)}\boldsymbol{r}^T\tilde{\boldsymbol{\Sigma}}^{1/2}\left(\boldsymbol{\Sigma}^{-1/2}\boldsymbol{S}^{-1}\boldsymbol{\Sigma}^{-1/2}\right)\boldsymbol{\Sigma}^{1/2}\tilde{\boldsymbol{r}} \\ &\quad = \frac{\hat{N}-m}{m}z^T\boldsymbol{W}^{-1}z \sim F\left(m, \hat{N}-m\right) \end{aligned} \tag{25}$$

Further,

$$T^2 \sim \frac{m\left(\hat{N}-1\right)\left(\hat{N}+1\right)}{\hat{N}\left(\hat{N}-m\right)} F\left(m, \hat{N}-m\right) \tag{26}$$

The detection criterion is as follows:

$$T^2 \begin{cases} \leq T_\alpha^2 & fault-free \\ > T_\alpha^2 & faulty \end{cases} \tag{27}$$

In order to compare the differences among different fault detection methods, the two important performance indicators are used, i.e., the false alarm rate (FAR) and the fault detection rate (FDR). The FAR can be given as follows [30]

$$\text{FAR} = \frac{N_{false-alarm}}{N_{fault-free}} \tag{28}$$

where $N_{false-alarm}$ is the number of the normal data sets misjudged as the fault and $N_{fault-free}$ is the number of the normal data sets. The FDR can be given as follows

$$\text{FDR} = \frac{N_{fault-detected}}{N_{faulty}} \tag{29}$$

where $N_{fault-detected}$ is the number of the fault data sets judged successfully and $N_{faulty}$ is the number of the fault data sets.

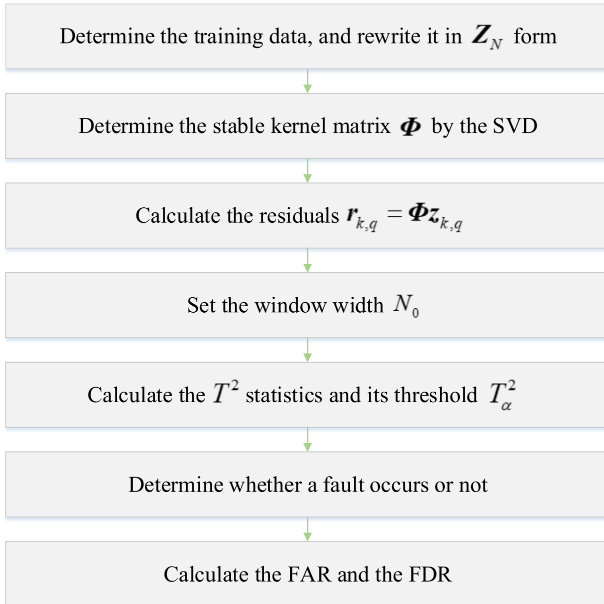


**FIGURE 1.** **The fault detection flow for the proposed method.**

### E. FAULT DETECTION FLOW

The algorithm steps for the fault detection in a closed-loop control system based on the parity space transformation are given in Fig. 1.

Step1. Determine the training data set and the number of the combination data $q$, and rewrite it in $\boldsymbol{Z}_N$ form according to Eq. (8);

Step2. Make the SVD of the data set, and use the rank and the unitary matrix to determine the stable kernel matrix $\boldsymbol{\Phi}$;

Step3. Calculate the residuals $\boldsymbol{r}_{k,q} = \boldsymbol{\Phi}z_{k,q}$ of the training data by using the stable kernel matrix $\boldsymbol{\Phi}$ and the data set $\boldsymbol{Z}_N$;

Step4. According to the method introduced in the Section IV-C, get the improved residuals by accumulating the $N_0$ residuals to increase the fault-to-noise;

Step5. According to Eq. (22) and Eq. (23), calculate the $T^2$ statistics by the improved residuals and the threshold $T_\alpha^2$;

Step6. Compare the $T^2$ statistic at each moment and the threshold $T_\alpha^2$ calculated with Eq. (23), and judge whether the fault occurs or not according to Criterion (27);

Step7. Determine $N_{false-alarm}$, $N_{fault-free}$, $N_{fault-detected}$ and $N_{faulty}$, and calculate the FAR and the FDR according to Eq. (28) and Eq. (29).

## V. SIMULATIONS

In this section, we report results of our simulations that verify the feasibility of the fault detection in the closed-loop control system based on the parity space transformation. The simulation cases include the numerical simulation model and the Tennessee Eastman Process (TEP) based on the industrial process simulation model.

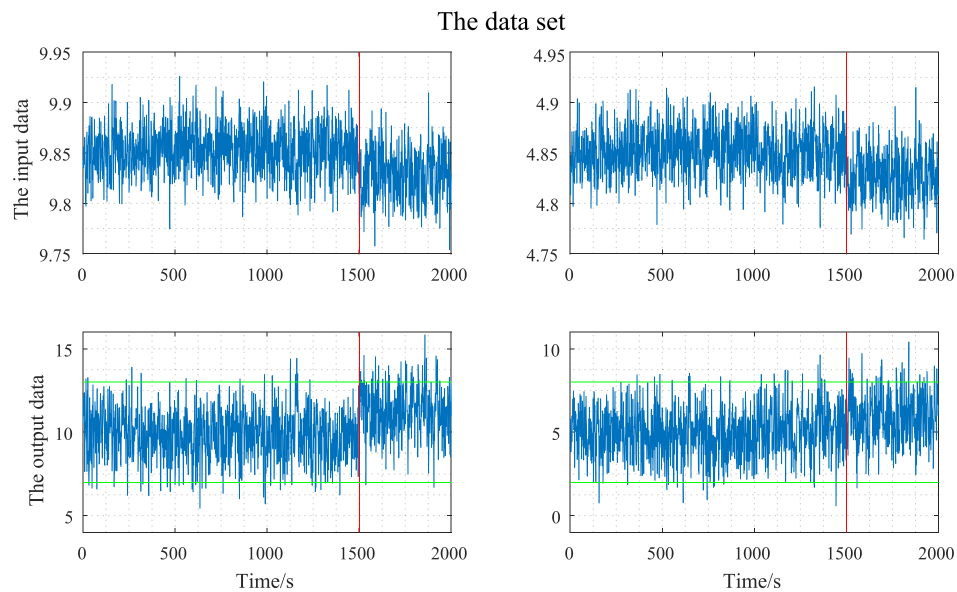


**FIGURE 2.** Simulation data set for the constant fault.

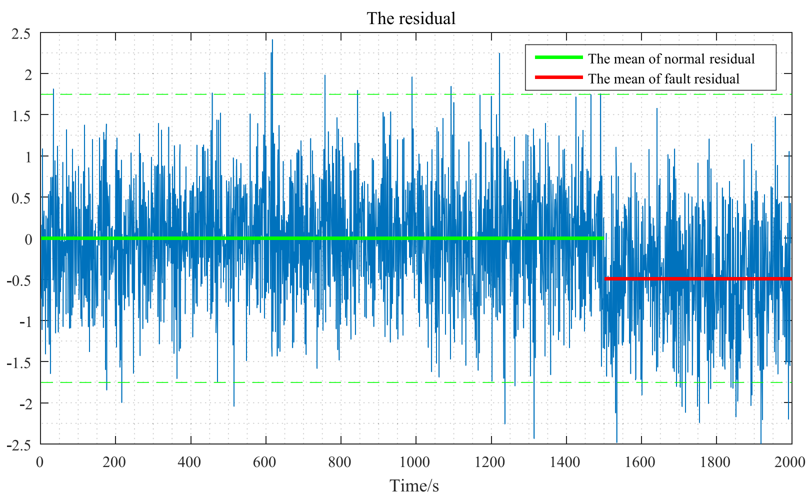


**FIGURE 3.** The detection residual by the parity space method.

### A. CASE 1: NUMERICAL SIMULATION MODEL

#### 1) EXAMPLE FOR DETECTING THE CONSTANT FAULT

The total amount of data is 2000 sets, in which the first 1000 sets of data are training data, the last 1000 sets of data are test data, and the first 1500 sets of data are fault-free, and the constant fault is added in the last 500 sets of data, and the fault magnitude is 1.5.

The dimension for both the input vector and the output vector is 2. The parameter matrices are $\boldsymbol{A} = 0.1\boldsymbol{I}_{2\times 2}$, $\boldsymbol{B} = 0.9\boldsymbol{I}_{2\times 2}$, $\boldsymbol{C} = \boldsymbol{I}_{2\times 2}$, $\boldsymbol{A}^c = \boldsymbol{I}_{2\times 2}$, $\boldsymbol{B}^c = \boldsymbol{0}$, $\boldsymbol{C}^c = \boldsymbol{I}_{2\times 2}$ and

$$\boldsymbol{D}^c = \begin{bmatrix} -0.01 & -0.01 \\ -0.01 & -0.01 \end{bmatrix},$$

respectively. The state noise and the measurement noise are independent with each other, and both obey the normal distribution with zero mean and the standard deviation is 1. The initial input values are set to 10 and 5, and the initial control values are also 10 and 5. Then the numerical simulation data set is obtained, as shown in 2.

In Fig. 2, the blue line represents the collected data set, and the part to the left side of the red line represents the normal operation of the system, and the part to the right indicates that the system fails, and the area between the two green lines indicates the normal operation of the system. It is obvious that when the constant fault occurs, the collected data is almost in the internal of $3\sigma$ range, hence it is difficult to effectively detect the constant fault using the traditional principles. According to the fault detection method based on the parity space in Section IV, the residuals are shown in Fig. 3.

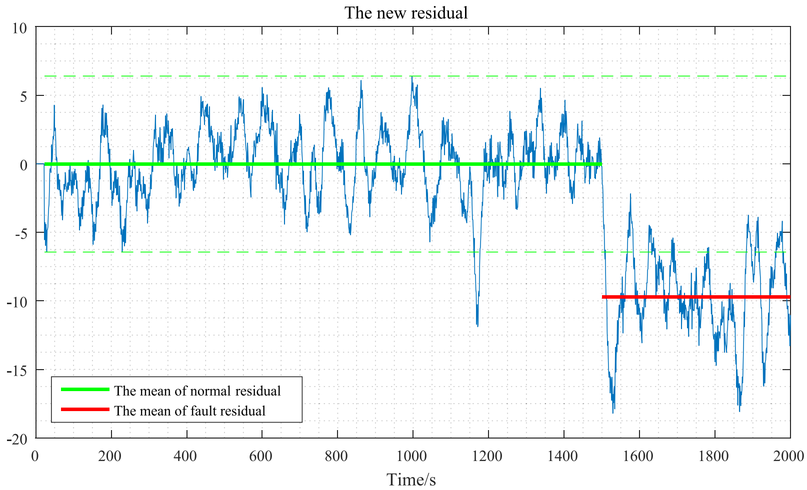


**FIGURE 4.** **The improved residuals by accumulating the data in the time window.**

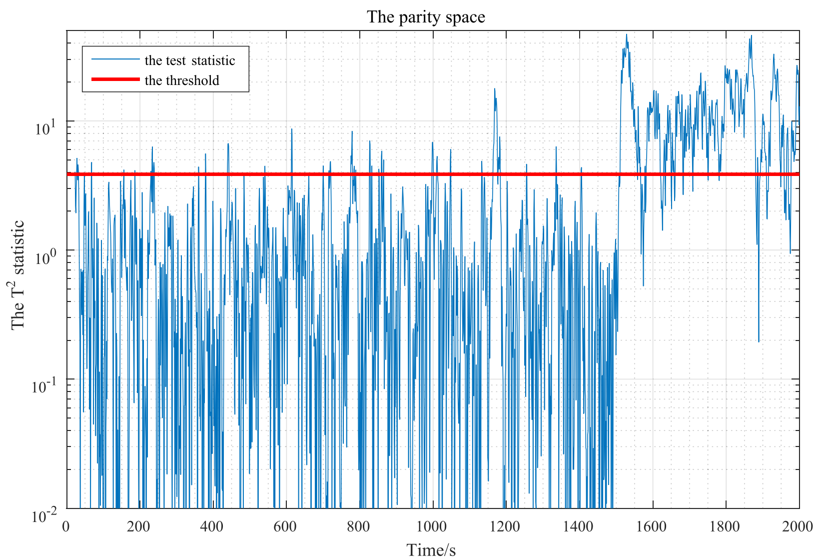


**FIGURE 5.** **The $T^2$ statistics based on the parity space.**

In Fig. 3, the green line represents the mean residual value when the system operates normally, and the red line represents the mean residual value of the system failure. According to the fault detection method in Section IV-C, we set the window width $N_0 = 20$, and the improved residuals are shown in Fig. 4.

According to Fig. 4, after the accumulation, the mean of the fault residual data deviates significantly from the mean of the normal residual data, in which the green solid line indicates the mean of the normal residual data, the red solid line indicates the mean value of the fault residual data, and the green dotted line indicates the $3\sigma$ range of the normal residual data. We can observe that there are more fault residuals outside of the $3\sigma$ range of the normal residual data, which can effectively improve the fault detection rate. According to the $T^2$ statistic and its threshold in Section IV-D, the detection result is shown in Fig. 5. According to Eq. (28) and Eq. (29), the FAR and the FDR can be calculated as FAR $= 0.0487$, FDR $= 0.9459$.

Using the same data, we computed the $T^2$ statistics based on the time series model and the result is shown in Fig. 6. The FAR and the FDR can be calculated as FAR $= 0.0537$, FDR $= 0.6593$.

We processed the same data by the PLS method, and the result is shown in Fig. 7. The FAR and the FDR can be calculated as FAR $= 0.0833$, FDR $= 0.6860$.

The comparison of the fault detection results for different methods is given in Table 1. The FAR is related to the significance level. From the table, we can see that the fault detection method based on the parity space transformation can significantly improve the fault detection performance.

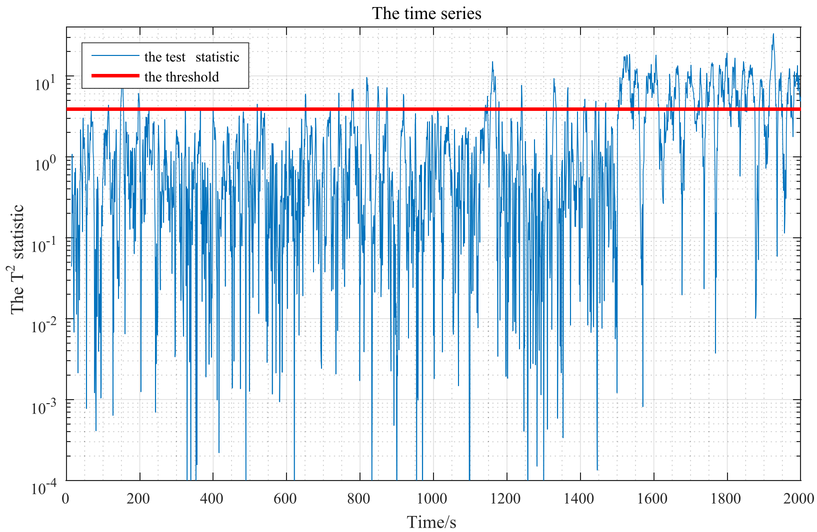


**FIGURE 6.** The $T^2$ statistics based on the time series.

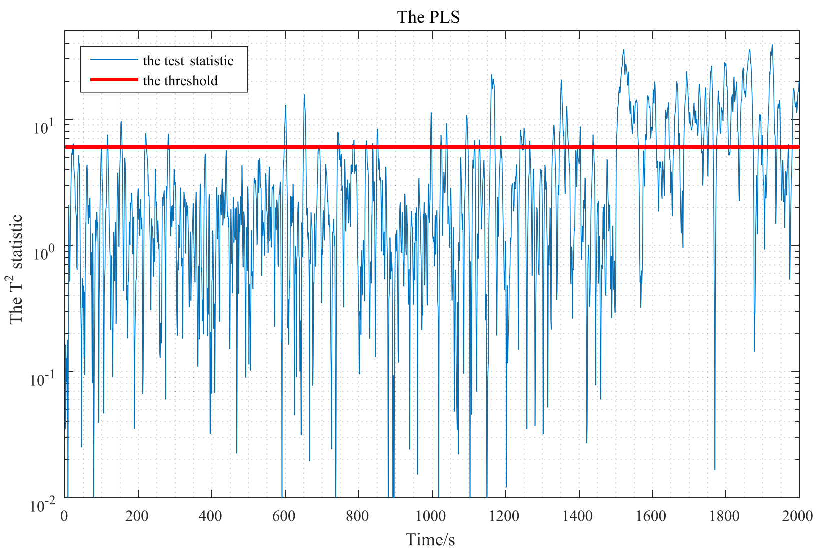


**FIGURE 7.** The $T^2$ statistics based on the PLS.

**TABLE 1.** The FAR and the FDR for different methods.

| Constant Fault Detection | Parity Space Method | Time Series Method | PLS Method |
|---|---|---|---|
| FAR | 0.0487 | 0.0537 | 0.0833 |
| FDR | 0.9459 | 0.6593 | 0.6860 |

In order to increase the fault-to-noise ratio, we proposed a new detection statistic by accumulating the residual sequence in the sliding window. We can see that window width has significant impact on the fault detection, including the fault detection rate and the detection delay. Table 2 shows the fault detection results obtained by the parity space transformation under different window widths.

As shown in Table 2, when the window width is 20, the fault detection rate exceeds 80%, and the detection delay is 18. Considering both the fault detection rate and the detection delay, it is acceptable to set the window width to 20 in this case.

In practical applications, the optimization selection window width is determined based on both the fault detection rate and the detection delay. For the general systems,

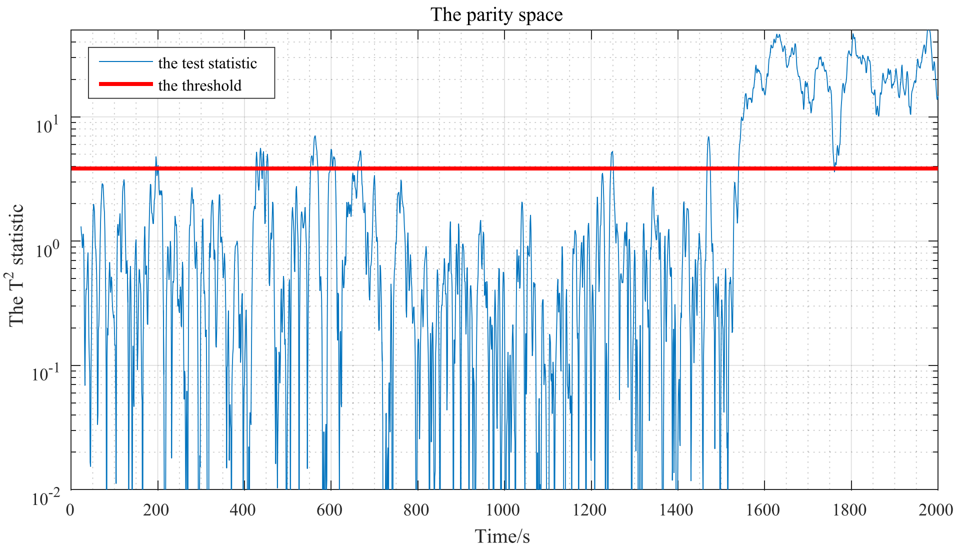


**FIGURE 8.** The $T^2$ statistics of the soft fault based on the parity space.

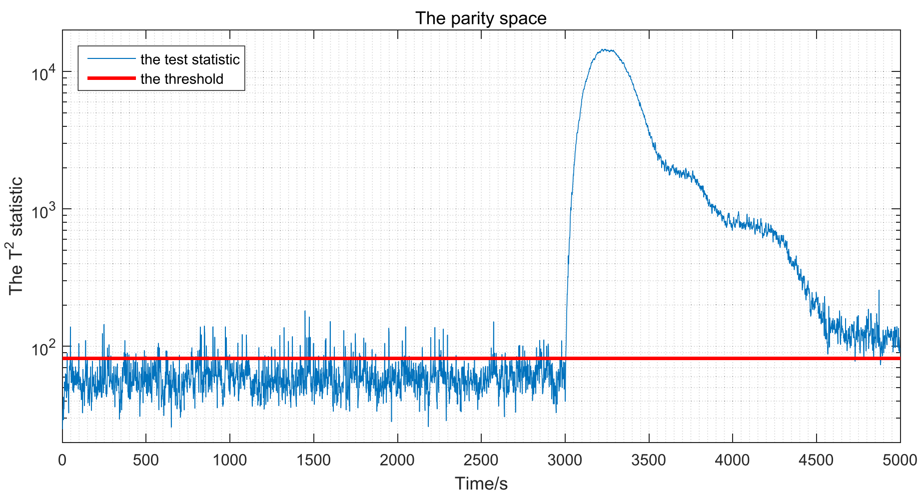


**FIGURE 9.** The $T^2$ statistics based on the parity space.

**TABLE 2.** Comparison of fault detection performance under different window widths.

| Window Width | Detection Performance based on Parity Space | | |
|---|---|---|---|
| | FAR | FDR | Detection Delay |
| 5 | 0.0576 | 0.5852 | 2 |
| 10 | 0.0625 | 0.7595 | 4 |
| 15 | 0.0526 | 0.8617 | 5 |
| 20 | 0.0487 | 0.9459 | 5 |
| 25 | 0.0611 | 0.9880 | 7 |
| 30 | 0.0626 | 0.9880 | 8 |

the fault detection rate can be improved by increasing the detection delay. While for high-risk complex systems with much stronger real-time requirement, the detection delay may be more concerned, and the delay needs to be appropriately reduced. In any case, our method provides a good way to adjust the performance.

### 2) EXAMPLE FOR DETECTING THE SOFT FAULT

If the fault mode is changed to the soft fault, that is, the data fault magnitude in the sample time range from 1501 to 1540 is slowly increased from 0 to 2, and the data fault magnitude in the sample time range from 2541 to 2000 is 2. Let the window width be $N_0 = 20$, based on the parity space transformation, the result is shown in Fig. 8:

The FAR and the FDR can be calculated as FAR $= 0.0541$, FDR $= 0.9218$. The FAR and the FDR obtained by different methods are shown in Table 3.

It can be seen from Table 1 and Table 3 that whether it is a constant fault or a soft fault, the proposed detection method

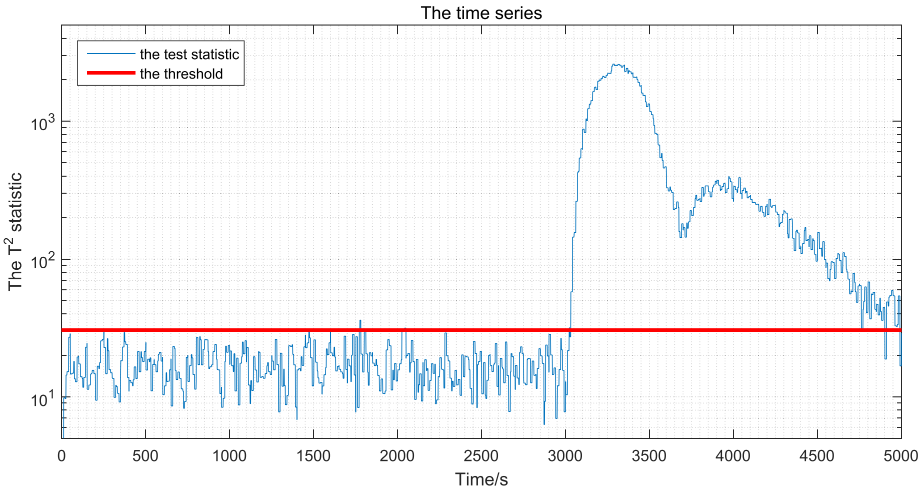


**FIGURE 10.** The $T^2$ statistics based on the time series.

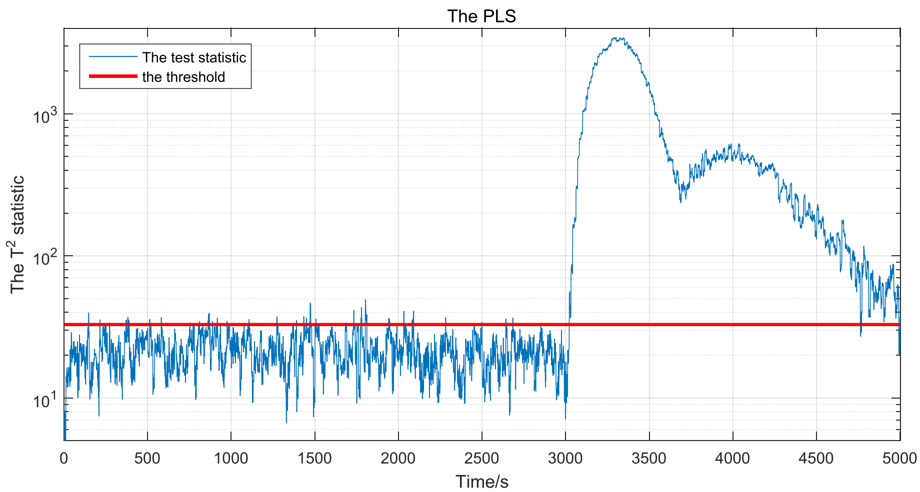


**FIGURE 11.** The $T^2$ statistics based on the PLS.

**TABLE 3.** The FAR and the FDR of different methods for the soft fault detection.

| | Parity Space Method | Time Series Method | PLS Method |
|---|---|---|---|
| FAR | 0.0460 | 0.0478 | 0.0435 |
| FDR | 0.9198 | 0.6258 | 0.6184 |

based on the parity space outperforms traditional methods with a higher fault detection rate.

### B. CASE 2: TEP SIMULATION MODEL

The Tennessee-Eastman Process (TEP) system is based on an industrial process simulation model that was created by an American company named Eastman in 1993, which can provide a realistic and usable industrial process for evaluating the process monitoring and control methods [30], [31]. The TEP system consists of five parts: reactor, condenser, compressor, steam/liquid separator and stripper. The equipment is operated under a closed-loop controller. A total of 41 variables are collected, of which the first 22 variables are the input data include feed, pressure, temperature, etc. The last 19 variables are the output data. In this experiment, the simulation time was set to 50 hours, the sampling period was 0.01 hours. Hence, in total, 5001 sets of data were sampled. The first variable was changed from the 30th hour to the end to set the fault. This data was used for the simulation experiment, and the first 2000 sets of data were used as the training data sets, and finally the false alarm rate and the fault detection rate were reported.

For this simulation, the result based on the parity space is shown Fig. 9. The FAR and the FDR can be calculated as FAR $= 0.0487$, FDR $= 0.9459$.

Similarly, the result based on the time series is shown in Fig. 10. The FAR and the FDR can be calculated as FAR $= 0.0537$, FDR $= 0.6593$.

Similarly, the result based on the PLS is shown in Fig. 11. The FAR and the FDR can be calculated as FAR $= 0.0833$, FDR $= 0.6860$.

**TABLE 4. The FAR and the FDR with different methods.**

| | Parity Space Method | Time Series Method | PLS Method |
|---|---|---|---|
| FAR | 0.0601 | 0.0067 | 0.0267 |
| FDR | 0.9945 | 0.9765 | 0.9830 |

The comparison of the detection results with different methods can be seen in Table 4. It is obvious that the fault detection based on the parity space outperforms both the time series method and the PLS method in the TEP system simulation.

### C. SIMULATION SUMMARY

From the above two experiments, we can conclude that the fault detection rate for the closed-loop control system using the proposed parity space transformation method is significantly higher than the time series method and the PLS method. There are two main reasons for this:

a) The parity space method can calculate the residual not in the original space, which can avoid the inaccurate fault detections caused by inaccurate estimation of the state vector;

b) A closed control loop system has strong robustness, and the original fault magnitude is partially offset. The time series method and the PLS method are used to obtain the residual by making the difference between the measured value and the predicted value, which will reduce the fault-to-noise ratio and the fault detection rate. However, the proposed parity space transformation method does not have such issues.

## VI. CONCLUSION

This paper has proposed a novel method based on parity space transformation for fault detection in closed-loop control systems. To achieve this, the characteristics of the closed-loop control system are analyzed, and the principle of the parity space is introduced. Then a straightforward fault detection method based on the parity space is designed, on top of which an improved method based on stable kernel matrix is further designed. In order to increase fault-to-noise ratios and improve fault detection rates, we have also proposed to accumulate residual sequence in a sliding window. Finally, the feasibility of the proposed method is verified by two simulation cases, which clearly confirms its superiority over traditional methods.

Our plans of future work include: (1) While our method in this work has focused on closed-loop control systems with linear control, actual complex systems tend to have strong nonlinear characteristics. Hence, we plan to address fault detection for closed-loop control systems with strong non-linearity in the near future. (2) Inside a closed-loop control system, a fault will generally propagate inside the system, which increases the difficulty for fault identification. We are also interested in addressing such issue in our future research.

## REFERENCES

[1] W. J. Wang and P. D. McFadden, "Application of wavelets to gearbox vibration signals for fault detection," *J. Sound Vibrat.*, vol. 192, no. 5, pp. 927–939, May 1996.
[2] M. Zhong, Y. Song, and S. X. Ding, "Parity space-based fault detection for linear discrete time-varying systems with unknown input," *Automatica*, vol. 59, pp. 120–126, Sep. 2015.
[3] Y. Xing, H. Wu, X. Wang, and Z. Li, "Survey of fault diagnosis and fault-tolerance control technology for spacecraft," *J. Astronaut.*, vol. 24, no. 3, pp. 221–226, May 2003.
[4] Z. D. and H. Y., "A review of fault diagnosis techniques for closed-loop systems," *Acta Automatica Sinica*, vol. 35, no. 6, pp. 748–758, 2009.
[5] A. Mahapatro and P. M. Khilar, "Fault diagnosis in wireless sensor networks: A survey," *IEEE Commun. Surveys Tuts.*, vol. 15, no. 4, pp. 2000–2026, 4th Quart., 2013.
[6] C. Sankavaram, B. Pattipati, K. R. Pattipati, Y. Zhang, and M. Howell, "Fault diagnosis in hybrid electric vehicle regenerative braking system," *IEEE Access*, vol. 2, pp. 1225–1239, 2014.
[7] C. Sankavaram, A. Kodali, K. R. Pattipati, and S. Singh, "Incremental classifiers for data-driven fault diagnosis applied to automotive systems," *IEEE Access*, vol. 3, pp. 407–419, 2015.
[8] H. Wang and X. Jing, "Fault diagnosis of sensor networked structures with multiple faults using a virtual beam based approach," *J. Sound Vibrat.*, vol. 399, pp. 308–329, Jul. 2017.
[9] S. Yin, X. D. Steven, A. Naik, P. Deng, and A. Haghani, "On PCA-based fault diagnosis techniques," in *Proc. Conf. Control Fault-Tolerant Syst.*, Oct. 2010, pp. 179–184.
[10] J. Li and P. Cui, "Improved kernel fisher discriminant analysis for fault diagnosis," *Expert Syst. Appl.*, vol. 36, no. 2, pp. 1423–1432, Mar. 2009.
[11] T. L. Schmitz, "Chatter recognition by a statistical evaluation of the synchronously sampled audio signal," *J. Sound Vibrat.*, vol. 262, no. 3, pp. 721–730, May 2003.
[12] Y.-X. Li and G.-H. Yang, "Fuzzy adaptive output feedback fault-tolerant tracking control of a class of uncertain nonlinear systems with nonaffine nonlinear faults," *IEEE Trans. Fuzzy Syst.*, vol. 24, no. 1, pp. 223–234, Feb. 2016.
[13] V. K. N. Lau, S. Cai, and A. Liu, "Closed-loop compressive CSIT estimation in FDD massive MIMO systems with 1 bit feedback," *IEEE Trans. Signal Process.*, vol. 64, no. 8, pp. 2146–2155, Apr. 2016.
[14] A. Bellini, F. Filippetti, G. Franceschini, and C. Tassoni, "Closed-loop control impact on the diagnosis of induction motors faults," *IEEE Trans. Ind. Appl.*, vol. 36, no. 5, pp. 1318–1329, Sep./Oct. 2000.
[15] J. Poon, P. Jain, I. C. Konstantakopoulos, C. Spanos, S. K. Panda, and S. R. Sanders, "Model-based fault detection and identification for switching power converters," *IEEE Trans. Power Electron.*, vol. 32, no. 2, pp. 1419–1430, Feb. 2017.
[16] Y. Cheng, R. Wang, and M. Xu, "A combined model-based and intelligent method for small fault detection and isolation of actuators," *IEEE Trans. Ind. Electron.*, vol. 63, no. 4, pp. 2403–2413, Apr. 2016.
[17] K. Turksoy, A. Roy, and A. Cinar, "Real-time model-based fault detection of continuous glucose sensor measurements," *IEEE Trans. Biomed. Eng.*, vol. 64, no. 7, pp. 1437–1445, Jul. 2017.
[18] A. Teixeira, I. Shames, H. Sandberg, and K. H. Johansson, "Distributed fault detection and isolation resilient to network model uncertainties," *IEEE Trans. Cybern.*, vol. 44, no. 11, pp. 2024–2037, Nov. 2014.
[19] H. H. Niemann and J. Stoustrup, "Robust fault detection in open loop vs. Closed loop," in *Proc. 36th IEEE Conf. Decision Control*, vol. 5, Dec. 1997, pp. 4496–4497.
[20] J. Wang and S. J. Qin, "Closed-loop subspace identification using the parity space," *Automatica*, vol. 42, no. 2, pp. 315–320, Feb. 2006.
[21] S. Zhao, B. Huang, and F. Liu, "Detection and diagnosis of multiple faults with uncertain modeling parameters," *IEEE Trans. Control Syst. Technol.*, vol. 25, no. 5, pp. 1873–1881, Sep. 2017.
[22] X. Zhang, W. Yan, X. Zhao, and H. Shao, "Nonlinear biological batch process monitoring and fault identification based on kernel fisher discriminant analysis," *Process Biochem.*, vol. 42, no. 8, pp. 1200–1210, Aug. 2007.
[23] S. Baek and D. Y. Kim, "Empirical sensitivity analysis of discretization parameters for fault pattern extraction from multivariate time series data," *IEEE Trans. Cybern.*, vol. 47, no. 5, pp. 1198–1209, May 2017.
[24] L. H. Chiang, E. L. Russell, and R. D. Braatz, *Partial Least Squares*, 2001.
[25] R. Muradore and P. Fiorini, "A pls-based statistical approach for fault detection and isolation of robotic manipulators," *IEEE Trans. Ind. Electron.*, vol. 59, no. 8, pp. 3167–3175, Aug. 2012.
[26] K. Wang, J. Chen, and Z. Song, "Data-driven sensor fault diagnosis systems for linear feedback control loops," *J. Process Control*, vol. 54, pp. 152–171, Jun. 2017.

[27] M. Zhong, S. X. Ding, Q.-L. Han, and Q. Ding, "Parity space-based fault estimation for linear discrete time-varying systems," *IEEE Trans. Autom. Control*, vol. 55, no. 7, pp. 1726–1731, Jul. 2010.

[28] Z. He, Z. Chen, H. Zhou, D. Wang, Y. Xing, and J. Wang, "A visualization approach for unknown fault diagnosis," *Chemometrics Intell. Lab. Syst.*, vol. 172, pp. 80–89, Jan. 2018.

[29] E. Lavretsky and K. A. Wise, *Advanced Textbooks in Control and Signal Processing*, 2013.

[30] Z. He, Y. A. W. Shardt, D. Wang, B. Hou, H. Zhou, and J. Wang, "An incipient fault detection approach via detrending and denoising," *Control Eng. Pract.*, vol. 74, pp. 1–12, May 2018.

[31] R. Eslamloueyan, "Designing a hierarchical neural network based on fuzzy clustering for fault diagnosis of the Tennessee—Eastman process," *Appl. soft computing*, vol. 11, no. 1, pp. 1407–1415, Jan. 2011.

**BOWEN SUN** was born in Siping, Jilin, China, in 1994. He received the B.S. degree in mathematics from the National University of Defense Technology, in 2017, where he is currently pursuing the master's degree.

He has authored more than five articles. His research interests include fault diagnosis, data processing, and data fusion.

**JIONGQI WANG** received the B.S. degree in applied mathematics from Zhejiang University, Hangzhou, China, in 2002, and the M.S. and Ph.D. degrees in system science from the National University of Defense Technology, in 2004 and 2008, respectively.

From 2008 to 2013, he was a Lecturer, and since 2014, he has been an Associate Professor with the College of Liberal Arts and Sciences, National University of Defense Technology, Changsha, China. He has published more than 40 refereed journal papers and eight international conference papers, coauthored three monographs and six patents. He conducts several outstanding research awards from the National Natural Science Foundation of China and Ministry of Education of China. His research interests include data driven diagnosis approaches, data processing, parameter estimation, system identification, and information fusion and its applications.

**ZHANGMING HE** received the B.S. and M.S. degrees in applied mathematics and the Ph.D. degree in system science from the National University of Defense Technology, Changsha, China, in 2008, 2010, and 2015, respectively. He is currently pursuing the Ph.D. degree with the Beijing Institute of Spacecraft System Engineering, China Academy of Space Technology.

From 2013 to 2014, he was a Visiting Scholar with the Institute for Automatic Control and Complex Systems, University of Duisburg-Essen, Duisburg, Germany. Since 2015, he has been a Lecturer with the College of Liberal Arts and Sciences, National University of Defense Technology.

He has published more than ten refereed journal papers and 15 international conference papers, coauthored two monographs and six patents. His research interests include fault diagnosis and prognosis, signal processing, and system identification.

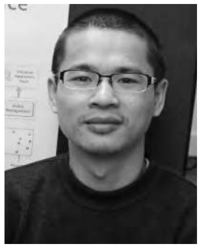

**YONGRUI QIN** received the B.S. and M.S. degrees from Fudan University, China, and the Ph.D. degree from the University of Adelaide, Australia, all in computer science.

During Ph.D. study, he spent six months as a Research Intern with DERI, Galway, Ireland (now The Insight Centre for Data Analytics). Since 2018, he has been a Doctoral Tutor with the School of Electronic Information Engineering, Guangdong University of Petrochemical Technology. He is currently a Senior Lecturer with the School of Computing and Engineering, University of Huddersfield, U.K. He has published more than 60 refereed technical papers, including publications in prestigious journals, such as *ACM Computing Surveys*, the IEEE Transactions on Parallel Distributed Systems, *ACM Transactions on Internet Technology*, *World Wide Web Journal*, the *Journal of Network and Computer Applications*, and the IEEE Internet Computing, as well as reputable international conferences, such as SIGIR, EDBT, CIKM, CAiSE, WISE, ICWS, SSDBM, and DASFAA. His current research interests include the Internet of Things, web of things, semantic web, data management, data mining, and mobile computing.

**DAYI WANG** received the Ph.D. degree in aerospace engineering from the Harbin Institute of Technology, in 2003.

From 2003 to 2015, he was a Researcher with the Beijing Institute of Spacecraft System Engineering, China Academy of Space Technology. From 2011 to 2015, he was the Deputy Director of the State Key Laboratory of Spatial Intelligent Control Technology and was the Chief Scientist for the 973-Project. He was authorized with 34 patents, published two monographs and more than 69 papers.

He received the National Outstanding Youth Fund of the National Natural Science Foundation of China. He conducted innovative research in the field of spacecraft autonomous navigation and control, solved a series of key technical issues and made great contributions to the success of key flight tests, such as the Chang'e-1 and the Chang'e-3 soft-landing probes.

**HAIYIN ZHOU** received the B.S. degree in applied mathematics from Wuhan University, Wuhan, China, in 1986, the M.S. degree from Hunan University, Changsha, China, in 1989, and the Ph.D. degree in systems engineering from the National University of Defense Technology, Changsha, China, in 2003.

Since 2009, he has been a Professor with the College of Liberal Arts and Sciences, National University of Defense Technology. He serves as a part-time Researcher with the Beijing Institute of Control Engineering, Beijing, China. He has published more than 80 refereed journal papers and ten international conference papers, coauthored four monographs and six patents. His research interests include data driven diagnosis approaches, power system dynamics and controls, advanced signal processing, and data information fusion and its application.